

# 1 Mapping the Wildland-Urban Interface in California: A Novel Approach based on 2 Linear Intersections

3 Mukesh Kumar\*<sup>1</sup> | Vu Dao<sup>1</sup> | Phu Nguyen<sup>1</sup> | Tirtha Banerjee<sup>1</sup>

4 <sup>1</sup>Department of Civil and Environmental Engineering, University of California, Irvine,  
5 CA 92697, USA

6 \*Corresponding author: Mukesh Kumar (mukeshk@uci.edu)

7  
8 The severity and frequency of wildfires have risen dramatically in recent years, drawing attention to the  
9 term 'wildland-urban interface' (WUI). WUI refers to the region where man-made constructions meet  
10 wildland vegetation. Existing conterminous United States (CONUS) WUI mapping methodologies were  
11 based on the intersection of the area of wildland vegetation and houses, rather than taking into account the  
12 direct physical contact of their boundaries. We mapped WUI in California (CA) based on the intersection  
13 of these boundaries using building footprint data rather than census block data and thus obtaining a finer-  
14 scale mapping. It is a point-based approach for WUI mapping and therefore, does not require accounting  
15 for the housing thresholds within a census block. This direct intersection of the housing and vegetation  
16 polygons is referred to as a direct WUI, whereas the intersection of the two polygon boundaries at 100 m  
17 is referred to as an indirect WUI. The linear WUI is a new WUI mapping that combines both direct and  
18 indirect WUI. We selected wildland vegetation polygons using NLCD 2016 data and Microsoft building  
19 footprint data for housing information. We chose shrubland, grassland, and woody vegetation types under  
20 the category of wildland vegetation. Our findings demonstrate that the direct WUI is less fragmented and  
21 has a slightly shorter length of 119,640 km than the indirect WUI (222,669 km) for the state of California.  
22 More fires were ignited closer to direct WUI than indirect WUI due to their proximity to communities.  
23 However, the overlap of past fire perimeters with indirect WUI is greater than that with direct WUI which  
24 shows that although more fires ignited in the direct WUI, they burned more areas in the indirect WUI due  
25 to embers transported by strong wind gusts during large wildfires. The study's findings will help land  
26 managers and policymakers in controlling fire dangers, planning land use, and reducing the threat to fire-  
27 prone communities.

28 **Keywords:** building footprint; California; linear WUI; wildfires; wildland vegetation; WUI

## 29 Plain Language Summary

30 In this study, we mapped linear WUI and defined direct and indirect WUI for California. Direct WUI has  
31 direct physical contact between flammable vegetation and housing boundaries and thus, has a higher risk

32 of fires due to human activities. While indirect WUI is mapped by the intersection of housing and a 100 m  
33 buffer boundary surrounding flammable vegetation and therefore, has a lower probability of wildfire.  
34 Results revealed that the direct WUI has a lower total length and is less fragmented than the indirect WUI  
35 in California. However, a higher percentage of fires are ignited in the vicinity of direct WUI because of the  
36 greater extent of human activities as compared to indirect WUI. Thus, even though direct WUI has a lower  
37 total length in California, it has a larger potential of fire ignitions in its proximity to historical sites of  
38 wildfires.

## 39 **1. Introduction**

40 The human propensity to live within the vicinity of natural amenities offered by forested lands and  
41 seashores has been recognized in past studies (Radeloff et al., 2001; Johnson et al., 2005; Bartlett et al., 2000).  
42 In the past few decades, there has been a dramatic proliferation in the number of regions where man-made  
43 structures are present within or near wildland vegetation, known as the Wildland-Urban Interface (WUI)  
44 (Radeloff et al., 2018; Martunizzi et al., 2015). This growth has been attributed to the increasing number of  
45 houses near forests and densely vegetated lands in the US since the mid-1900s (Radeloff et al., 2018,  
46 Martunizzi et al., 2015). In recent years, the term WUI has gained tremendous popularity and has been  
47 widely used in the context of wildfires. For the purpose of a more accurate analysis of the wildfire  
48 occurrences, tracking the location of wildfires, and land use planning, different WUI mapping  
49 methodologies have been developed in the past using a wide range of datasets across many countries  
50 including Europe, Australia, and Canada (Hanberry et al., 2020; Miranda et al., 2020; Bento-Gonçalves et  
51 al., 2020). A few studies have used point-based house locations, while others have implemented a zone-  
52 based approach such as census block data for WUI mapping (Radeloff et al., 2005; Wilmer and Aplet, 2005).  
53 In addition, these maps also depend on the context and purpose of the study; for example, housing-centric  
54 or fuel-centric WUI mapping, as demonstrated in Stewart et al., 2009. WUI maps in Canada show that these  
55 features could be also developed for different types of man-made structural regions, and a recent study  
56 mapped wildland industrial interface for dense industrial locations, as well as for urban and infrastructural  
57 interfaces (Johnston et al., 2018).

58 In the US, WUI mapping was based on the 2001 federal register definition of the US Department  
59 of Interior (US DOI) and the US Department of Agriculture (USDA) which states that WUI are those areas  
60 where houses are present within or nearby wildland vegetation. In the original definition, it was not  
61 specified whether the intersection of these two types of land use were based on the intersected area or the  
62 common boundary of two polygons. However, previous studies were based on areal intersection, i.e., in

63 terms of intersection of the area of these two features. Therefore, the resulting WUI had units in sq. m with  
64 a dimension in [L<sup>2</sup>]. In addition, past WUI maps focused on providing WUI areas and did not account for  
65 the length of the interface. Moreover, the past WUI maps were based on zonal approaches where either a  
66 housing density was defined or point based approaches where individual housing locations were used.  
67 These approaches lacked consistency on accurate information on all three components of the WUI  
68 definition together - accurate housing information, accurate vegetation information and a clear definition  
69 of the interface and the proximity of buildings to large vegetated areas.

70 To address this gap, Pereira et al., 2018 argued that a semantically correct definition of an interface  
71 (Webster's Third New International Dictionary (Gove, 1961)) should be a plane or other surface forming a  
72 common boundary of two bodies or spaces. Therefore, ideally, the result of WUI mapping would be a line  
73 segment that could show the common boundary or the physical contact between the boundaries of two  
74 features. Linear WUI offers greater simplicity in the storage and utilization of information over previous  
75 WUI mappings because each WUI line segment can be tagged with information about its surroundings,  
76 such as distance to nearby roads, fuel types, population, building and vegetation density, etc. (Pereira et  
77 al., 2018). Indeed, this novel approach would be very helpful in the identification of important physical  
78 features such as adjacent fuels, topography, nearby roadways, and other infrastructures from the linear  
79 WUI. The new WUI map for CA will yield a more accurate analysis of the wildfire events with respect to  
80 WUI as it maps at a 30-m finer-scale resolution. Furthermore, the statistical analysis based on these new  
81 maps and past wildfires would help future development, land use planning, and locating the high-risk  
82 sites. The distance between previous wildfire ignition points and WUI line will show how far wildfires  
83 occurred from the linear WUI. This would help in the identification of the wildfire risk prone areas. It is  
84 expected that more ignitions near the linear WUI segments due to human ignited fires. In addition, the  
85 wildfire burned area with respect to the WUI line segment will provide more information on the severity  
86 of the fire as well as the respective risk level.

87 The resulting linear WUI features from this approach will be in vector format as opposed to rasters,  
88 which have been provided by the previous WUI mapping approaches. In geospatial analysis, vector data  
89 are associated with higher geographic accuracy because of lesser dependence on grid size. Additionally,  
90 storing, handling, and appending new data layers to vector data is significantly more efficient compared  
91 to rasters which are considerably larger in size. In addition, vector data are much more scalable, amenable  
92 to defining connections between topology and network structures, and easier for delineating boundaries  
93 and administrative maps in fine resolution, comparable to raster datasets. Moreover, storing of vector data  
94 is possible without the loss of generalization and preserving geolocation information. Therefore, it is

95 envisioned that developing wildland fire policies under a changing climate and growing trends in WUI  
96 land use features will be more efficient using linear WUI features as developed in this manuscript.

97 Wildland fires destroy thousands of buildings in the US annually. In recent years, CA wildfires  
98 have burned the highest number of acres of all states in the US, according to the National Interagency Fire  
99 Center (NIFC) report (2018). This wildfire season gained the title of 'giga fire' in the year 2020 and burned  
100 more than a million acres of land compared to previous years during which the burned area had been  
101 recorded as a few hundred thousand acres ('mega fire'). In 2020, 4,177,855 acres of California burned with  
102 a total of 9,639 wildfire incidents that destroyed 10,488 buildings and caused 33 fatalities according to the  
103 2020 CAL FIRE summary report. In the same year, out of nearly 17,700 total damaged structures in the US,  
104 11,253 buildings were destroyed and affected by wildfires in CA which made it one of the most devastating  
105 wildfire seasons on record. From 2010 to 2020, a total of 52,955 buildings were destroyed in CA on its own  
106 (Headwater economics, November 2020: [https://headwaterseconomics.org/natural\\_hazards/structures-  
107 destroyed-by-wildfire/](https://headwaterseconomics.org/natural_hazards/structures-destroyed-by-wildfire/)). The biodiversity of nature was affected with the total extinction of a few species  
108 of flora and fauna in the local and regional forested lands. Whenever homes are constructed near flammable  
109 vegetation, it poses two types of major issues: first, the risk of human sparked fires increases, and second,  
110 it also escalates the risk of damage caused by wildfires (Radeloff et al., 2018). Recent studies suggest that  
111 most of the CA wildfires destroyed houses in the WUI but occurred outside the existing WUI regions  
112 (Kumar et al., 2020; Kramer et al., 2018). It is therefore important to analyze how far the linear WUI features  
113 are present from the past wildfire events and would be helpful in monitoring fires in proximity to these  
114 linear WUIs, as well as in making development plans in the immediate area.

115 This paper contributes in a number of ways to existing WUI literature. To the authors' knowledge,  
116 this paper is one of the first attempts to map the linear WUI for the US using a point-based approach, i.e.,  
117 the location of individual buildings at a finer resolution of 30 m and linear features. This means that rather  
118 than providing the areas that WUIs contain, the focus of this mapping approach is the boundaries that  
119 mark the edges of the interface, which is semantically more accurate. This novel WUI map gives the most  
120 accurate representation of the intersecting boundaries between the flammable vegetation and houses. This  
121 map will guide local and regional government agencies to determine the location of infrastructures for  
122 further construction and development of buildings, roads, and power supplies, etc. Furthermore, it would  
123 also help in locating the highly risky areas where there are many communities living nearby these WUI  
124 lines and thus policies and activities will be implemented in a way to either reduce the density of houses  
125 or clear the fuel loading in such regions. Findings from this study will be helpful for wildfire management  
126 and will benefit policymakers and land managers at the state and local levels. More specifically, it will help

127 to focus on the WUI line segments which will determine the nearby high-risk prone areas for future  
128 wildfires, help in land use planning and reduce risk of damages from severe wildfires to the communities  
129 living in the vicinity of flammable vegetation.

130 The key objectives of this study are as follows: (i) map the linear WUI in terms of direct and indirect  
131 interfaces and determine which WUI is more widespread in CA; (ii) evaluate how much percentage of  
132 wildfires occurred in the linear WUI features in CA; (iii) examine the distance between wildfire ignition  
133 points and the linear WUI features to see how far the fires ignited from it since 2010 in CA. Thus, this paper  
134 aims to show the importance of the novel linear WUI features for CA at both the local and federal level.  
135 This paper is organized as follows. Data and methodology that are used to generate WUI maps for CA are  
136 presented in section 2. Section 3 describes the results and discussions of our novel linear WUI calculations  
137 using building footprint datasets. Finally, conclusions and implementation of this study are given in section  
138 4.

## 139 **2. Data and Methodology**

### 140 **2.1. Vegetation data**

141 The vegetation data used for this study was Landsat-based, the 2016 National Land Cover Database  
142 (NLCD) (Jin et al., 2019), a new generation of NLCD products, released by the U.S. Geological Survey  
143 (USGS). It was designed specifically for the rapidly growing demand for land cover change analysis and  
144 the related studies, and it represented the most robust land cover base ever produced by the USGS. It  
145 included land cover and its changes over the CONUS for seven years, 2001, 2003, 2006, 2008, 2011, 2013,  
146 and 2016. Thus, it increased the land cover time series from 10 years to 15 years (2001 to 2016) (Homer et  
147 al., 2020). It was downloaded from Multi-Resolution Land Characteristics (MRLC) Consortium (available  
148 on <https://www.mrlc.gov/>) and was available at 30 m spatial resolution. The accuracy and robustness of  
149 the NLCD 2016 map were also shown by recent studies including Jin et al., 2019 and Homer et al., 2020.  
150 NLCD 2016 could be used for the identification of the different features at a finer resolution and thus can  
151 be considered for the deeper analysis of the expanding areas and further planning of the developmental  
152 activities. It contained a total of 28 different types of land cover classes over the CONUS. For the purpose  
153 of mapping the linear WUI, we chose only those vegetation categories which were flammable vegetation  
154 and included shrubland, grassland, woody wetlands, and all kinds of forest vegetation (California fire  
155 alliance 2001; Radeloff et al., 2005). Specific steps used for extracting the vegetation layer using ArcMap  
156 tools will be discussed in methodology section 2.4.

### 157 **2.2. Building data**

158 With the improvement of remote sensing data in acquisition efficiency and resolution, it has become  
159 possible to extract detailed housing boundaries from it. Over the past few years, Microsoft has made great  
160 efforts in applying deep learning, computer vision, and Artificial Intelligence for mapping, and leveraging  
161 the power of Machine Learning in analyzing satellite imagery to trace the shape of buildings across the  
162 country. More specifically, Bing Maps, a mapping platform from Microsoft had successfully generated the  
163 first comprehensive high-quality housing footprints database covering the entire CONUS by using Deep  
164 Neural Network (DNN) and the residual neural network (ResNet34) with segmentation techniques (Refine  
165 Net up-sampling) to detect individual building footprints from their imagery data. However, there was a  
166 need to develop some methodologies to put this data in a more usable format for the researchers and land  
167 planning management, to study and analyze the human and environmental impacts on small cities and  
168 regions (Heris et al., 2020; Demuzere et al., 2020). A new method of rasterizing building footprint was  
169 developed by Heris et al., 2020 and was used in this study to produce a robust WUI map. Taking advantage  
170 of the new building dataset from Microsoft product and rasterizing method, we propose a new framework  
171 of mapping novel linear WUI over California. The building dataset was extracted from the Microsoft  
172 dataset containing 124,885,597 computer-generated building footprints in GeoJSON format for the US.  
173 Regarding the accuracy metrics, the precision of the evaluation set is 99.3 % and the recall is 93.5 %. The  
174 California building footprint file implemented in this study contained 10,988,525 computer-generated  
175 building footprints in California and was extracted from the US building footprint dataset by Microsoft  
176 (2018), then converted to shapefile format. We used a rasterized format of Microsoft building footprint  
177 datasets, available at 30 m spatial resolution, and used the boundaries of houses for producing the linear  
178 WUI feature (Heris et al., 2020; Li et al., 2021). This boundary data was obtained from Heris et al., 2020 in  
179 which the value of each cell represents the area of the cell that was covered by building footprints. The cell  
180 values were calculated by developing an algorithm that used High Performance Computing (HPC) (Heris  
181 et al., 2020). This algorithm created a small meshgrid (a 2D array) for each building's bounding box,  
182 generating unique values for each meshgrid cell that was further coordinated with NLCD products to make  
183 it more usable (projected using Albers Equal Area Conic system) (Heris et al., 2020). The range of values  
184 was from 0 to 900 sq. meters. To better aid the implementation of building footprint data into large-scale  
185 computation, these values are represented as raster layers with a 30 m cell size covering each of the 48  
186 conterminous states.

187

### 188 **2.3. Wildfires data**

189 Previous wildfire data were downloaded from Monitoring Trends in Burn Severity (MTBS), (available  
190 on <https://www.mtbs.gov/direct-download>). MTBS is an interagency initiative whose purpose is to  
191 continuously monitor the intensity of wildfires in terms of burn severity and the size of major fires from  
192 1984 to present in the US. It does not cover small fires and includes all those fires in the Western US of 1000  
193 or more acres, and 500 or greater acres in the Eastern part of the US (MTBS, 2021). In this study, we used  
194 two kinds of MTBS datasets, namely, wildfire occurrence dataset that showed wildfire ignition points, and  
195 burned area boundaries datasets, representing wildfire perimeters. For analyzing the overlap of previous  
196 wildfires with the linear WUI features, we used wildfire perimeter. While detecting the distance of previous  
197 wildfire events from the linear WUI features, we used wildfire ignition points data. Since the liner WUI  
198 was mapped using the recent land cover and housing information, therefore, to better analyze the WUI  
199 maps and their relationship with the previous wildfires, we included only those fires which occurred in  
200 the last decade i.e., from 2010 to 2018. It shows all 380 fire perimeters of all fire events that happened in  
201 California from 2010 to 2018 and are represented by the legend in Figure 3.

202

#### 203 **2.4. Methodology**

204 NLCD data was clipped for California from the CONUS. Clipped land cover data was converted to  
205 polygons from the original raster data using the conversion tool from the ArcGIS geoprocessing. A  
206 wildland vegetation layer was generated for WUI mapping using selection by attributes from the attribute  
207 table using ArcGIS. Only shrub/grassland, herbaceous, woody wetlands, emergent herbaceous wetlands,  
208 and forests including evergreen, mixed, and deciduous were selected for the wildland vegetation layer  
209 (Radeloff et al., 2005; Martunizzi et al., 2015). The building raster layers were converted into vectors. The  
210 boundaries of the building were intersected with the wildland vegetated areas to map the wildland-urban  
211 interface. The resulting feature is a line, called direct WUI or indirect WUI at a 100-m buffer distance from  
212 the building boundary.

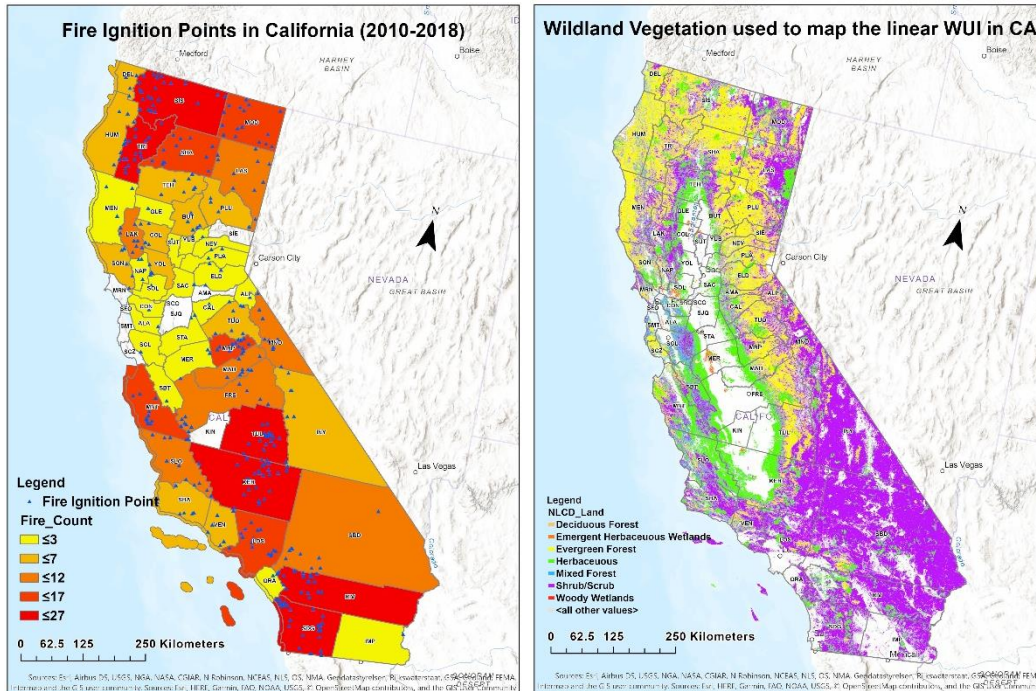
213 Direct WUI was calculated using the intersection tool from ArcMap using the vegetation polygon and  
214 housing boundary, and it represents the direct physical contact of buildings with the flammable vegetation.  
215 There is always a higher risk of damage to the communities living at the direct WUI feature as compared  
216 to those living at the indirect WUI as studied by Pereira et al., 2018. To map the indirect WUI, first, we took  
217 a buffer distance of 100-m from the vegetation polygon and then extracted those areas in California which  
218 had neither buildings nor vegetation using the erase tool from ArcMap. We then intersected the extracted  
219 layer with the buffered vegetation layer. Finally, we intersected the previously intersected layer with the

220 housing boundary to get the Indirect WUI. We did not intersect the vegetation layer with a buffer and  
221 housing boundary to avoid the repetition/duplication of indirect WUI lines with the direct WUI. The  
222 resulting WUI, both direct and indirect, have units of length in meters (m) with [L]<sup>1</sup> dimension.

### 223 3. Results and Discussions

#### 224 3.1. Wildland fire ignition frequency

225 A total of 380 wildfires occurred in California from 2010 to 2018 as reported by MTBS. These included  
226 both man-made fires as well as fires ignited by natural causes, such as lightning. In the left panel of Figure  
227 1, we show the countywide fire frequency in California, with more than 20 large fires in some of the  
228 counties, as shown with the red colorbar. We observe that northernmost and southern California have the  
229 highest number of fires (Figure 1, left panel). Notably in southern California, the counties of San Diego  
230 (SDG) and Kern (KER) each had 27 fires from 2010 to 2018. While in the northern part, Siskiyou (SIS) County  
231 had a maximum of 24 fires during the same period. Strong wind events, more specifically, Diablo winds in  
232 northern California and Santa Ana winds in southern California are the main drivers for the larger and  
233 more devastating wildfires. Furthermore, human ignition is one of the most significant factors in the last  
234 few decades for a majority of the deadliest fires. Counties with zero wildfires were shown with no color  
235 and thus left blank white spaces, as can be referred to in the left panel of Figure 1. A few counties had no  
236 or very few wildfire events during 2010-2018; however, these counties more recently recorded severe  
237 wildfires that are not shown here. For example, the Silverado fire occurred in October and November 2020  
238 in southern Orange County, California. However, such wildfire occurrences are not included in this study  
239 because of the unavailability of adequate datasets for the recent wildfire events.



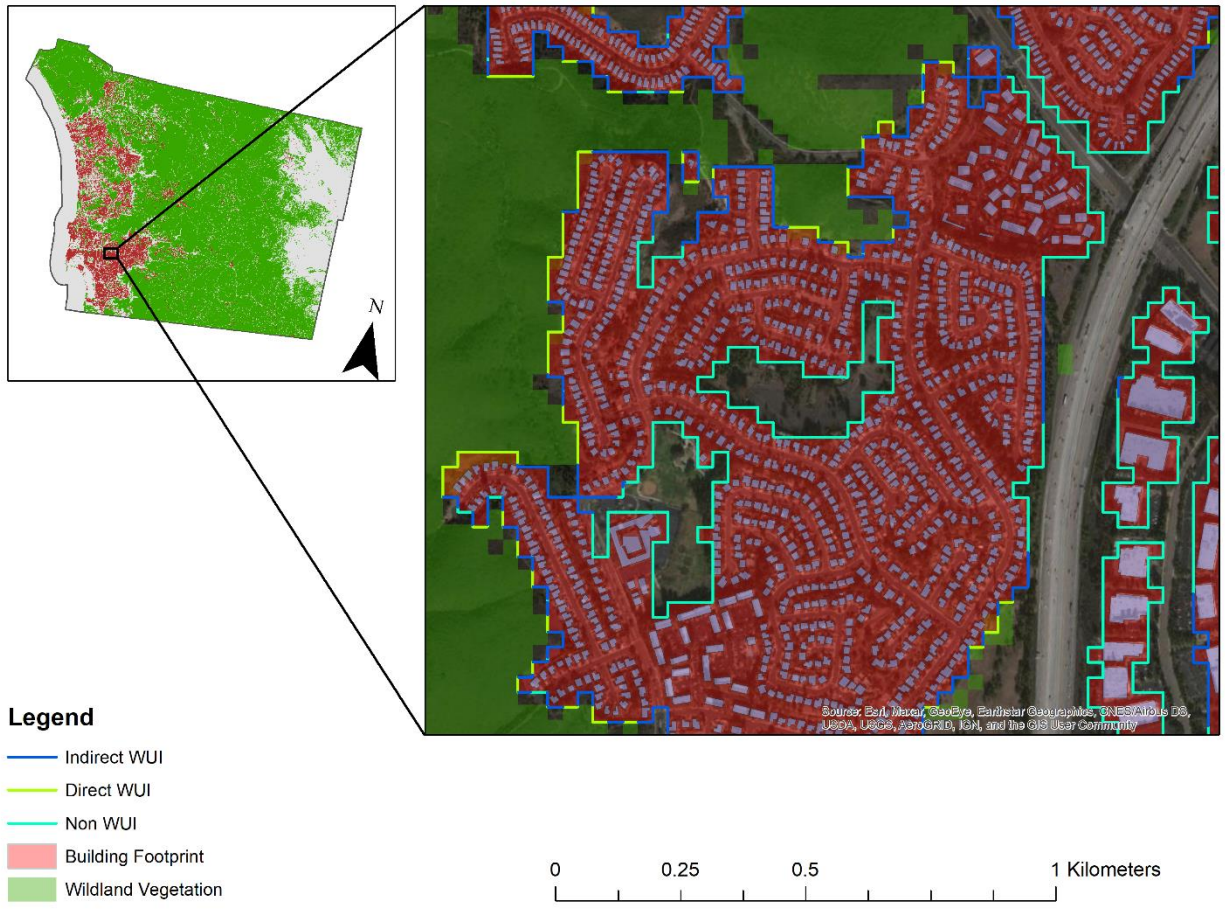
240  
 241 **Figure 1.** The left panel on the figure above shows wildfire frequency in all the counties of California from  
 242 2010 to 2018. The blue triangular-shaped symbols represent the wildfire ignition points in the respective  
 243 counties, while the colorbar shows the number strength of these fire frequencies for each County. The white  
 244 portions of the map represent those counties where the fire activity was absent. The right panel on the  
 245 figure above shows the spatial pattern of NLCD data, the wildland vegetation data used to map the linear  
 246 WUI for California at 30 m resolution; it includes three kinds of forest, shrubs, and emergent herbaceous &  
 247 woody wetlands; white color represents the water bodies and other vegetation types that were not included  
 248 for mapping the linear WUI.

249 Figure 1 (right panel) depicts the wildland vegetation cover used in the mapping of linear WUI. This  
 250 map clearly shows that the majority of southern California is covered by shrubland vegetation, whereas  
 251 the dominant land cover type in the north is evergreen forest and shrubland. Furthermore, the variability  
 252 in land cover type is greater in the northern counties of California than in the southern regions. Overall,  
 253 shrubland is the most common type of vegetation in California. Shrublands are defined as ecosystems with  
 254 a minimum of 30% shrub or sub-shrub cover and tree densities of up to 10 trees per hectare (USDA). They  
 255 are one of the significant regions where wildfire season lasts the longest (Jolly et al., 2015). Although it has  
 256 a low fuel presence, those available fuels are very dry and therefore, the fire spread is very high in  
 257 shrublands (Bond et al., 2001). Also, recent studies have shown that the shrublands are one of the areas

258 most affected by wildfires (Jolly et al., 2015). The white colorbar in the right panel of Figure 1 also reflects  
259 water and other land cover types that are not classified as wildland vegetation while mapping linear WUI.

260 **3.2. Linear WUI features in California**

261



263 **Figure 2.** The left panel on the figure above shows the spatial pattern of Microsoft building footprints and  
264 vegetation data in San Diego. A section of the County map has been enlarged to depict the direct, indirect,  
265 and non-WUI lines as well as their actual visualization at 30 m resolution. This is displayed in the right  
266 panel of the figure above.

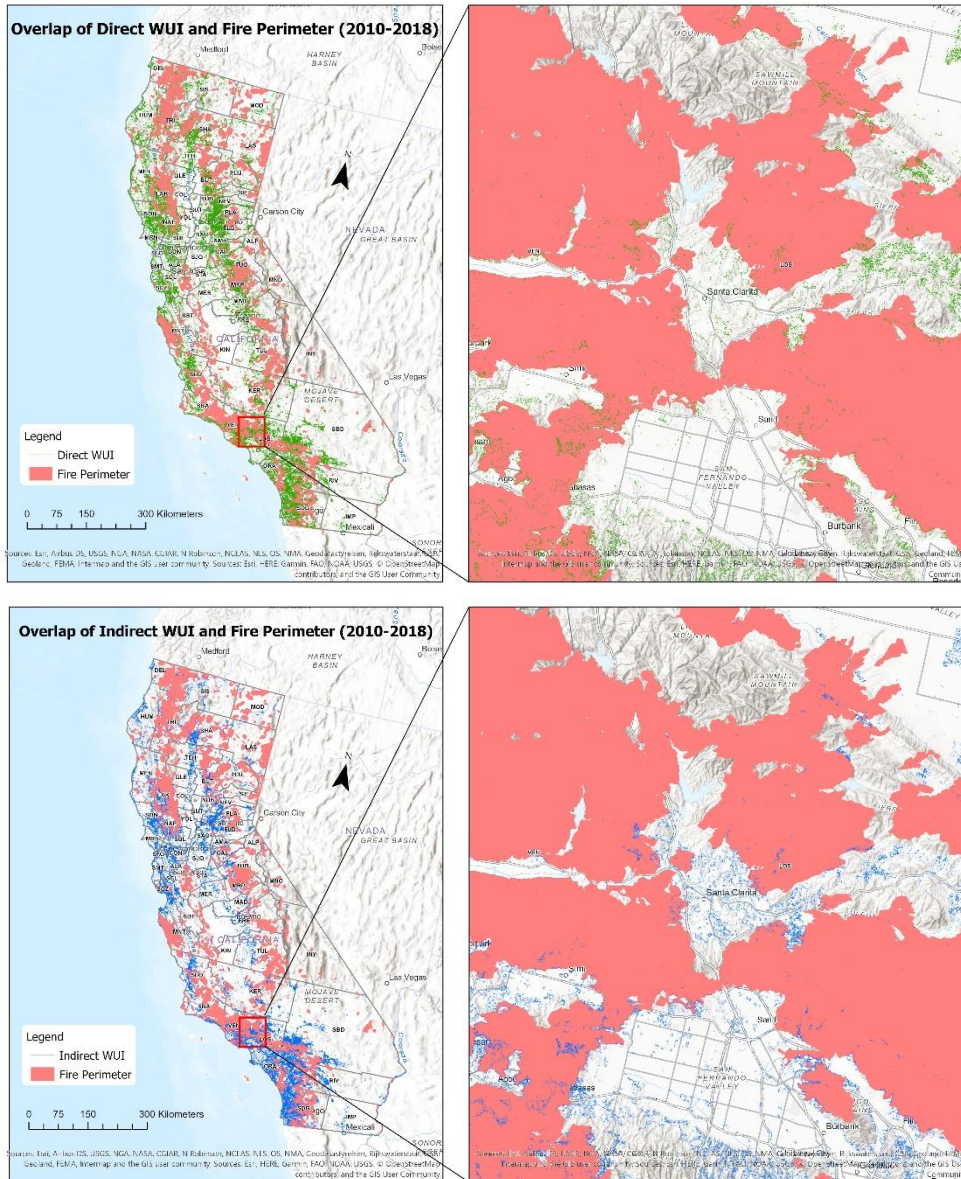
267 Direct WUI is a linear WUI feature that is shown in Figure 2, with pixel lengths in meters (m) and is  
268 represented with a green colorbar. Enlarged portion of Figure 2 on the right panel depicts a very clear  
269 visualization of the different linear WUI (direct and indirect WUI) and Non-WUI segments and it became  
270 possible only due to the finer-scale mapping using building footprint data at 30-m resolution. In addition,  
271 such a finer-scale WUI map provides more detailed information related to both housing and wildland

272 vegetation. Linear WUI segments may be used to gather information about building density, population  
273 and the area of the housing cluster. Similarly, it can also be used to collect data related to flammable  
274 vegetation, such as, area of the flammable patch, types of near fuel availability, and proximity to roads, etc.  
275 The findings of this analysis will help foresters, land managers, and policymakers plan future development  
276 activities, mitigation, and evacuation. Most importantly, by shrinking the linear WUI, the risk of  
277 community damage can be reduced. It can be achieved by either clearing off flammable vegetation nearby  
278 buildings or slowing down the rate at which new houses are being built near flammable vegetation.

279

### 280 3.3. Overlap of wildfires and linear WUI

281

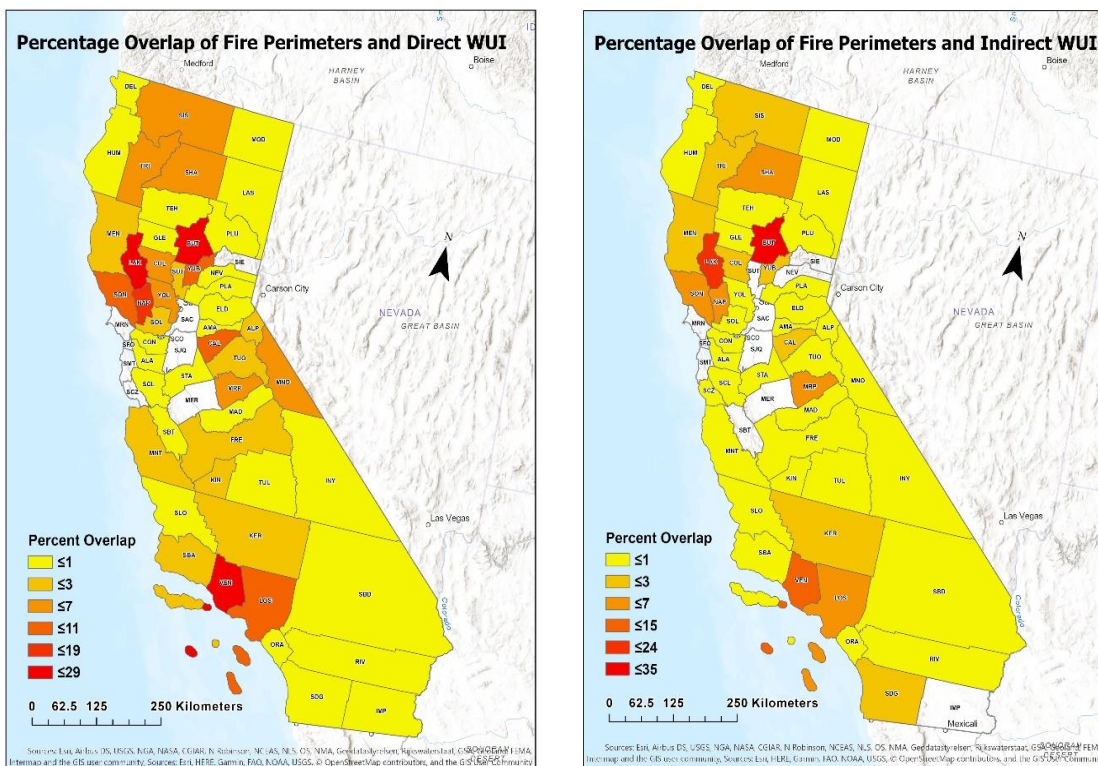


282 **Figure 3.** The figure shows the overlap of California historic wildfire perimeters (2010-2018) with direct  
283 WUI (top left panel) and indirect WUI (top right panel). Legends with green and blue lines represent direct  
284 and indirect WUI respectively in the above figure. The right-hand panels present enlarged views of the  
285 relevant sections of the two maps for clearer visualization.

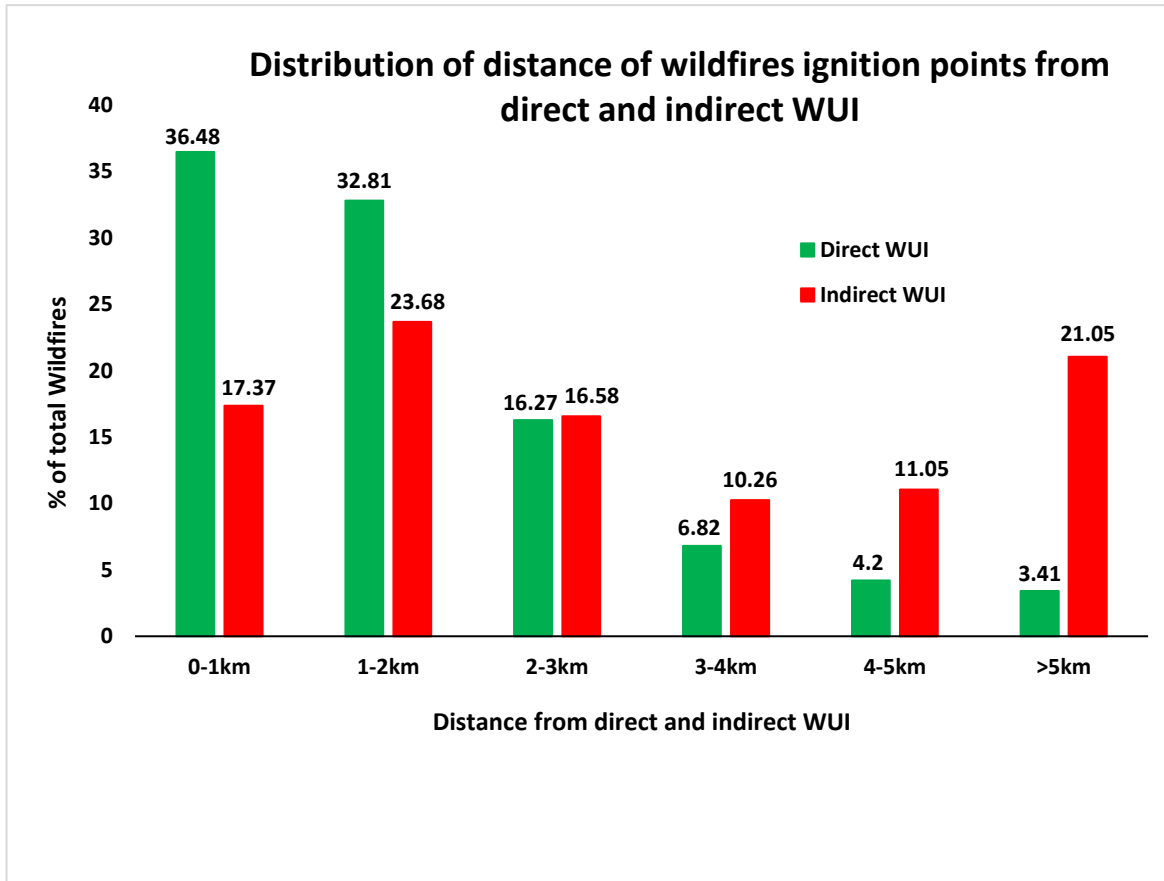
286 Figure 3 depicts the overlap of wildfire perimeters with direct WUI from 2010 to 2018. This result  
287 clearly indicates that there is a very low percentage of overlap between the direct WUI and the fire  
288 perimeters. However, a maximum of up to 29 % of all direct WUI lines in California overlap within the past  
289 wildfire perimeters (left panel, Figure 4). Thus, the results show that the majority of wildfires are not  
290 occurring at WUI lines and may be burning farther away from the direct WUI lines. Similarly, a  
291 considerable percentage of fires ignited and burned outside WUI areas, according to a recent study by  
292 Kumar et al., 2020. In the case of indirect WUI, though, the percentage overlap between indirect WUI and  
293 wildfire perimeters is still low, but it is higher than what we have seen with direct WUI (Figure 4). Because  
294 of the devastating wildfire in Butte County in 2018, i.e., the Camp Fire, the maximum value of percentage  
295 overlap rises up to 35%. The percentage overlap of wildfire perimeters and indirect WUI might vary  
296 depending on how we choose the wildland vegetation perimeters when mapping the indirect WUI.

297 We calculated that the total pixel length of direct WUI in California is 119,640,741 m. It has 672,435  
298 counts with a maximum count length of 5,958 m. In contrast, indirect WUI has a total pixel length of  
299 164,706,030 m, which comprises a total number of 3,009,978 counts, with the highest length of a count being  
300 5,022 m. When we examined these two linear WUI features, we discovered that the direct WUI has a lower  
301 total pixel length than the indirect WUI. However, a higher percentage of fires ignited in close proximity  
302 to direct WUI as compared to those in the vicinity of indirect WUI (Please refer to Table S1 in the  
303 supplementary materials). As a result, even though direct WUI has a lower total pixel length in California,  
304 it has a larger potential of fire ignitions in its vicinity based on prior fire incidence data. In addition, the  
305 maximum length of a count, the statistical parameters like mean, median, and mode are higher for the  
306 direct WUI. However, the total number of counts is lower for direct WUI as compared to indirect WUI. As  
307 a result, this difference in counts reveals that the direct WUI is less fragmented than the indirect WUI  
308 (Figure 3). A greater length of linear WUI in a region corresponds to a higher likelihood of wildfire risk  
309 due to the presence of flammable vegetation nearby. Moreover, a greater length of linear WUI also indicates  
310 a larger number of interfaces between flammable vegetation and human settlements which would mean a  
311 higher risk of damage to the lives, properties, and health of a larger number of communities nearby that  
312 region. As mentioned earlier, the direct WUI indicates direct physical contact between houses and  
313 flammable vegetation. Hence, the likelihood of fire ignition increases as one gets closer to these linear WUI

314 features. Interestingly, from 2010 to 2018, 36.58 % of wildfires in California were ignited within 1 km of  
 315 direct WUI, according to our assessment. In the case of indirect WUI, it represents an indirect contact  
 316 between the housing boundary and flammable vegetation, with a 100-meter buffer surrounding it (Pereira  
 317 et al., 2018). As a result, we analyzed those house boundaries that do not cross directly with flammable  
 318 vegetation, and we expected that there would be a lower likelihood of wildland fires in the presence of  
 319 such linear WUI characteristics as compared to direct WUI. Indeed, we revealed in our analysis that only  
 320 17.37 % of fires ignited within 1 km of indirect WUI. As a result, we can see that there are lower risks of  
 321 wildfire ignitions closer to indirect WUI than to direct WUI.  
 322



323 **Figure 4.** The figure shows the countywise percentage overlap of total direct WUI (left panel) and total  
 324 indirect WUI (left panel) of California with wildfire perimeters from 2010 to 2018. Colorbar shows the  
 325 increase from yellow (low) to red (high) for the respective counties in California.  
 326

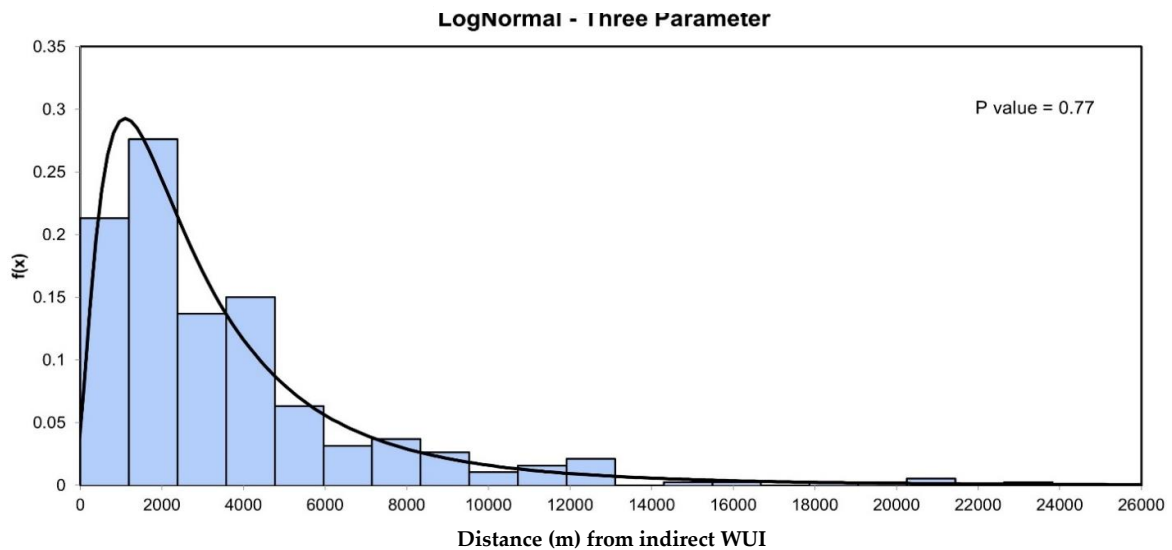
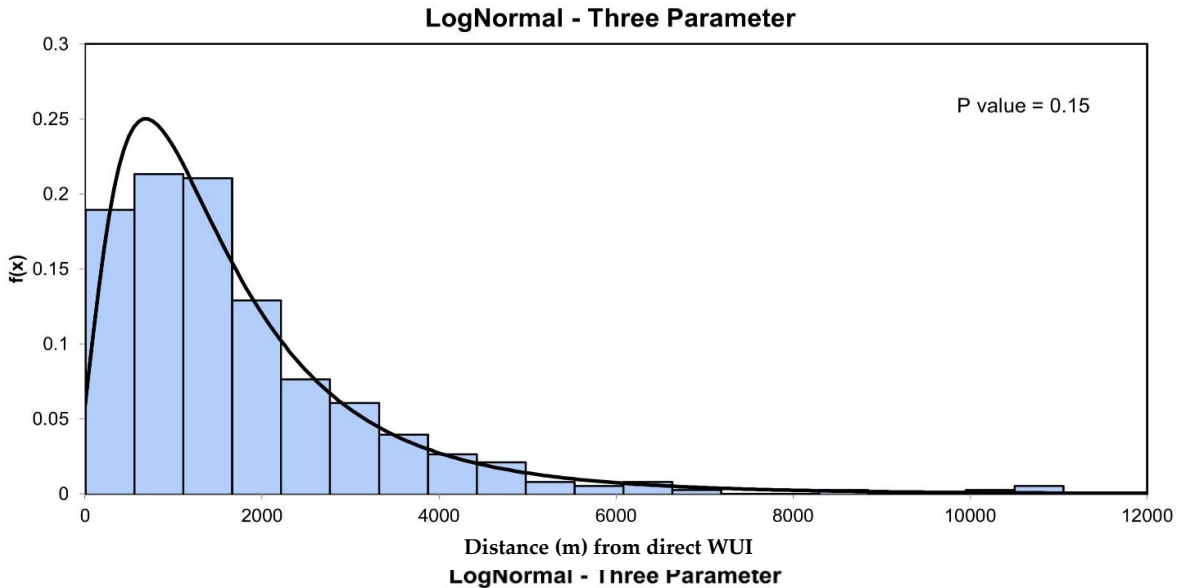


328

329 **Figure 5.** The figure shows two histograms for the distribution of distance of wildfire ignition points on the  
 330 either side from linear WUI features. Histogram for the direct WUI (green) shows a continuous decreasing  
 331 percentage of wildfires; while it is neither continuously increasing nor continuously decreasing and has  
 332 two peaks for the indirect WUI (red).

333 In Figure 5, we show the histogram plots for the distribution of distance of wildfire ignition points in  
 334 six different classes from the direct, and indirect WUI respectively. Additionally, the percentages, total  
 335 number of fires that occurred between these classes are also shown. In our analysis, we observe that in case  
 336 of the direct WUI, 139 fires ignited out of a total of 380 fires i.e., 36.58% of fires ignited within 1 km range  
 337 on either side from direct WUI (Please also refer to Table S1 in supplementary materials). It has decreased  
 338 continuously as we increase the distance farther away from the direct WUI. And it dropped to only 3.42 %  
 339 of total fires that were ignited above 5 km distance from the direct WUI in California (Figure 5). In case of  
 340 indirect WUI, we found a different trend of the fire ignitions in different classes of the distance ranges on  
 341 either side of the indirect WUI. Only 90 fires ignited within 1 km distance on either side of the indirect

342 WUI, making it 17.37% fires within this range (Please also refer to Table S1 in supplementary materials).  
343 However, it has increased from 17.37% to 23.68% in the range of 0-1 km to 1-2 km distance from indirect  
344 WUI features respectively (Figure 5). Additionally, a significant portion of the fires i.e., 21.05% ignited  
345 above 5 km on either side from the indirect WUI. And this accounts for 80 fires out of a total 380 fires that  
346 ignited above 5 km in California from 2010 to 2018. We can indeed conclude that the direct WUI is more  
347 prone to fire activity based on the past nine years of wildfire history in California. And, thus, there is a  
348 higher risk of damage due to wildland fires within the closer proximity of direct WUI. On the other hand,  
349 almost 83% of fires ignited above 1 km distance from the indirect WUI. Therefore, there is lower probability  
350 of burning within 1 km distance from the indirect WUI as compared to the direct WUI. Additionally, a  
351 significant percentage of fires ignited above 5 km distance from the indirect WUI as compared to the direct  
352 WUI.



353 **Figure 6.** The figure shows the distribution of the best fit plot for distance (m) of wildfire ignition points  
354 from direct WUI (top panel) and indirect WUI (bottom panel).

355 It is crucial to observe how far fires ignited from the linear WUI features and which statistical curve  
356 will best fit the distribution of the distance between fires and WUI. Therefore, we performed the statistical  
357 analysis and used different curve fittings to choose the best fit curve for both direct and indirect WUI. We  
358 chose 13 different distributions to test the best fit as shown in Table S2 in the supplementary information.  
359 Our analysis reveals that the 'lognormal with three parameters' distribution is the best fit curve for the  
360 direct WUI as can be seen in the top panel of Figure 6. It has a p-value of 0.15 that is highest of all, as  
361 compared to the p values of the other 12 distributions (Please refer to Table S2 in supplementary materials).  
362 In this approach the null hypothesis is that the dataset is sampled from the chosen distribution and a p-  
363 value larger than the significance level 0.05 indicates that the null hypothesis cannot be rejected in favor of  
364 the alternate hypothesis. Apart from p-value, there are other parameters to check whether or not the result  
365 of a statistical analysis is adequate. For example, the location and scale of a distribution also tells us about  
366 the data structure. The scale parameter describes how spread out the data values are, while the location  
367 parameter describes how large the data values are. However, some of the distributions like 'weibull' and  
368 'gamma' do not have these parameters (Please refer to Table S2 in supplementary materials). And therefore,  
369 we must check for the 'shape' parameter, which is an outcome of these distributions. The shape parameter  
370 describes how the data is spread. In general, a larger scale results in a more spread-out distribution. In this  
371 study, we used a suitable number of datasets (380) to perform the statistical analysis in both direct and  
372 indirect WUI (Please refer to Table S2 in supplementary materials). Therefore, the conclusion of our results  
373 based on p value is adequate and acceptable. As we can see in the bottom panel of Figure 6, lognormal with  
374 three parameters is also the best fit curve in the case of indirect WUI.

#### 375 **4. Conclusions**

376 Past studies showed that different WUI maps were developed for the CONUS using a variety of  
377 datasets and different mapping methodologies. However, neither of these focused on WUI mapping based  
378 on the linear intersection of vegetation and housing boundary, using building footprint and NLCD land  
379 cover data respectively. In this study, we mapped linear WUI at 30 m resolution. We defined two types of  
380 linear WUI i.e., direct, and indirect WUI for California. Direct WUI has direct physical contact between  
381 flammable vegetation and housing boundary and thus, has a higher risk of fires. While indirect WUI is  
382 mapped by the intersection of housing, and 100 m buffer boundary surrounding flammable vegetation and  
383 therefore it has a lower probability of fires. Results revealed that the direct WUI had a lower total pixel

384 length and is less scattered than the indirect WUI in California. However, a higher percentage of fires  
385 ignited in the vicinity of direct WUI because of a higher extent of human activities as compared to indirect  
386 WUI. Hence, even though direct WUI has a lower total pixel length in California, it has a larger potential  
387 of fire ignitions in its vicinity based on the historical wildfires. Furthermore, the majority of wildfires did  
388 not burn along WUI lines, and we found that the overlap between wildfire burned areas and WUI hardly  
389 goes up to 30% for some of the counties. The reason for this is simply because some of the recent fires  
390 occurred over these linear WUIs. Furthermore, the percentages are lower in most of the counties in  
391 California as wildfires did not burn directly over it, but in the vicinity of linear WUI features. As revealed  
392 in this study, 69.47% fires ignited within 2 km range from direct WUI and 41.05% ignited within the same  
393 range from indirect WUI in California. Therefore, in this study, we show that the direct WUI are more  
394 prone to wildfires as compared to the indirect WUI. Not only this but also, the fires ignited from the linear  
395 WUI features follow a 'lognormal with three parameters' distribution in both direct and indirect WUI.  
396 Results from this study show that most of the wildfire events in CA have occurred within 2 km linear  
397 distance from these linear WUI features and this study also proposes that fires are not happening at the  
398 intersecting lines, but they ignite farther away from the linear WUI features as highlighted in Kumar et al.,  
399 2020. These linear WUI maps will help in creating and sustaining a fire-adapted community within a WUI.  
400 This would also help policymakers to develop a community wildfire protection plan in the era of climate  
401 change that will bring an increase in wildfire events in the future. In addition, it will enhance community  
402 awareness regarding the prevention of fires within the WUI. Overall, this research will help in creating a  
403 more effective response to the wildfire events that will occur in the WUI.

#### 404 **Acknowledgments**

405 M. Kumar and T. Banerjee acknowledge the funding support from the University of California Laboratory  
406 Fees Research Program funded by the UC Office of the President (UCOP), grant ID LFR-20-653572.  
407 Additional support was provided by the new faculty start up grant provided by the Department of Civil  
408 and Environmental Engineering, and the Henry Samueli School of Engineering, University of California,  
409 Irvine.

#### 410 **Author Contributions**

411 **Mukesh Kumar:** Conceptualization, Methodology, Software, Data curation, Writing- Original draft  
412 preparation, Visualization, Investigation, Software, Validation, Writing-Reviewing and Editing; **Vu Dao:**

413 Investigation, Visualization; **Phu Nguyen**: Methodology, Software; **Tirtha Banerjee**: Conceptualization,  
414 Supervision, Reviewing and Editing, Project administration, Funding acquisition.

#### 415 **Conflicts of Interest**

416 The authors declare no conflict of interest.

#### 417 **References**

418 Bartlett, J.G., Mageean, D.M. and O'Connor, R.J., 2000. Residential expansion as a continental threat to US  
419 coastal ecosystems. *Population and Environment*, 21(5), pp.429-468.

420 Bento-Gonçalves, A. and Vieira, A., 2020. Wildfires in the wildland-urban interface: Key concepts and  
421 evaluation methodologies. *Science of the total environment*, 707, p.135592.

422 Bond, W. Fires, Ecological Effects of. In *Encyclopedia of Biodiversity*, Volume 2; Academic Press:  
423 Cambridge, MA, USA, 2001; pp. 745–753.

424 Demuzere, M., Hankey, S., Mills, G., Zhang, W., Lu, T. and Bechtel, B., 2020. Combining expert and crowd-  
425 sourced training data to map urban form and functions for the continental US. *Scientific data*, 7(1), pp.1-13.

426 Glickman, D. and Babbitt, B., 2001. Urban wildland interface communities within the vicinity of federal  
427 lands that are at high risk from wildfire. *Federal Register*, 66(3), pp.751-777.

428 Gove, P. B. (1961). *Webster's Third New International Dictionary of the English Language*, unabridged. (P.  
429 B. Gove, Ed.). Springfield, Mass.: G&C Merriam Company.

430 Hanberry, B.B., 2020. Reclassifying the Wildland–Urban Interface Using Fire Occurrences for the United  
431 States. *Land*, 9(7), p.225.

432 Headwater Economics, November 2020: [https://headwaterseconomics.org/natural-hazards/structures-  
433 destroyed-by-wildfire/](https://headwaterseconomics.org/natural-hazards/structures-destroyed-by-wildfire/)

434 Heris, M.P., Foks, N.L., Bagstad, K.J., Troy, A. and Ancona, Z.H., 2020. A rasterized building footprint  
435 dataset for the United States. *Scientific Data*, 7(1), pp.1-10.

436 Homer, C., Dewitz, J., Jin, S., Xian, G., Costello, C., Danielson, P., Gass, L., Funk, M., Wickham, J., Stehman,  
437 S. and Auch, R., 2020. Conterminous United States land cover change patterns 2001–2016 from the 2016  
438 national land cover database. *ISPRS Journal of Photogrammetry and Remote Sensing*, 162, pp.184-199.

439 Jin, S., Homer, C., Yang, L., Danielson, P., Dewitz, J., Li, C., Zhu, Z., Xian, G. and Howard, D., 2019. Overall  
440 methodology design for the United States national land cover database 2016 products. *Remote*  
441 *Sensing*, 11(24), p.2971.

442 Johnson, K.M., Nucci, A. and Long, L., 2005. Population trends in metropolitan and nonmetropolitan  
443 America: Selective deconcentration and the rural rebound. *Population Research and Policy Review*, 24(5),  
444 pp.527-542.

445 Johnston, L.M. and Flannigan, M.D., 2018. Mapping Canadian wildland fire interface areas. *International*  
446 *journal of wildland fire*, 27(1), pp.1-14.

447 Jolly, W.M., Cochrane, M.A., Freeborn, P.H., Holden, Z.A., Brown, T.J., Williamson, G.J. and Bowman,  
448 D.M., 2015. Climate-induced variations in global wildfire danger from 1979 to 2013. *Nature*  
449 *communications*, 6(1), pp.1-11.

450 Kramer, H.A., Mockrin, M.H., Alexandre, P.M., Stewart, S.I. and Radeloff, V.C., 2018. Where wildfires  
451 destroy buildings in the US relative to the wildland–urban interface and national fire outreach programs.  
452 *International Journal of Wildland Fire*, 27(5), pp.329-341.

453 Kramer, H.A., Mockrin, M.H., Alexandre, P.M. and Radeloff, V.C., 2019. High wildfire damage in interface  
454 communities in California. *International journal of wildland fire*, 28(9), pp.641-650.

455 Li, S., Dao, V., Kumar, M., Nguyen, P. and Banerjee, T., 2021. Mapping the wildland-urban interface in CA  
456 using remote sensing data. ESSOAR Preprints, doi: 10.1002/essoar.10507343.3

457 Martinuzzi, S., Stewart, S.I., Helmers, D.P., Mockrin, M.H., Hammer, R.B. and Radeloff, V.C., 2015. The  
458 2010 wildland-urban interface of the conterminous United States. *Research Map NRS-8. Newtown Square, PA:*  
459 *US Department of Agriculture, Forest Service, Northern Research Station. 124 p.[includes pull-out map]., 8*, pp.1-  
460 124.

461 Miranda, A., Carrasco, J., González, M., Pais, C., Lara, A., Altamirano, A., Weintraub, A. and Syphard, A.D.,  
462 2020. Evidence-based mapping of the wildland-urban interface to better identify human communities  
463 threatened by wildfires. *Environmental Research Letters*, 15(9), p.094069.

464 Monitoring Trends in Burn Severity (2019) Monitoring Trends in Burn Severity (MTBS). Available at  
465 <http://www.mtbs.gov/>.

466 M. Kumar, S. Li, P. Nguyen, T. Banerjee, ESSOAr (2020). Revisiting the existing definitions of wildland-  
467 urban interface for California. doi/10.1002/essoar.10504449.1

468 National Interagency Fire Center (NIFC), 2018 and 2019 report.

469 Pereira, J., Alexandre, P., Campagnolo, L., Bar Massada, A., Radeloff, V. and Silva, P., (2018). Defining and  
470 mapping the wildland-urban interface in Portugal. *VD Xavier: Advances in Forest Fire Research*, pp.743-  
471 749

472 Radeloff, V.C., Hammer, R.B., Voss, P.R., Hagen, A.E., Field, D.R. and Mladenoff, D.J., 2001. Human  
473 demographic trends and landscape level forest management in the northwest Wisconsin Pine  
474 Barrens. *Forest Science*, 47(2), pp.229-241.

475 Radeloff, V.C., Hammer, R.B., Stewart, S.I., Fried, J.S., Holcomb, S.S. and McKeefry, J.F., 2005. The  
476 wildland–urban interface in the United States. *Ecological applications*, 15(3), pp.799-805

477 Radeloff, V.C., Helmers, D.P., Kramer, H.A., Mockrin, M.H., Alexandre, P.M., Bar-Massada, A., Butsic, V.,  
478 Hawbaker, T.J., Martinuzzi, S., Syphard, A.D. and Stewart, S.I., 2018. Rapid growth of the US wildland-  
479 urban interface raises wildfire risk. *Proceedings of the National Academy of Sciences*, 115(13), pp.3314-3319.

480 Stewart, S.I., Wilmer, B., Hammer, R.B., Aplet, G.H., Hawbaker, T.J., Miller, C. and Radeloff, V.C., 2009.  
481 Wildland-urban interface maps vary with purpose and context. *Journal of Forestry*, 107(2), pp.78-83.

482 Stewart, S.I., Radeloff, V.C., Hammer, R.B. and Hawbaker, T.J., 2007. Defining the wildland–urban  
483 interface. *Journal of Forestry*, 105(4), pp.201-207.

484 Wildfire Today, 2020. Available at [https://wildfiretoday.com/2020/09/21/community-destruction-during-  
485 extreme-wildfires-is-a-home-ignition-problem/](https://wildfiretoday.com/2020/09/21/community-destruction-during-extreme-wildfires-is-a-home-ignition-problem/)

486 Wilmer, B. and Aplet, G., 2005. Targeting the community fire planning zone: Mapping matters. *The  
487 Wilderness Society: Washington, DC, USA*.

488

489

490

491

492

493

494

495

### Supplementary Information

496 **Table S1.** Statistical summary table showing distance of fire ignition points with respect to direct and  
497 indirect WUI in California.

498

Distance from Indirect WUI (km)	No. of wildfires (2010-2018)		Percentage of total fires (%)	
	Indirect	Direct	Indirect	Direct
0-1	66	139	17.37	36.58
1-2	90	125	23.68	32.89
2-3	63	62	16.58	16.05
3-4	39	26	10.26	6.84
4-5	42	16	11.05	4.21
>5	80	13	21.05	3.42

499

500

501

502

503

504

505 **Table S2.** Statistical analysis using 13 different curve fittings to choose the best fit curve for the distribution  
 506 of the distance between wildfire ignition points and WUI line segments (direct & indirect WUI).

507

508

Curve fitting summary table for direct WUI

Descriptive Statistics									
	Count	Mean	StDev	Median	Min	Max	Skew	Kurt	
	380	1741.6	1554.6	1425.9	4.689	11056	2.388	9.107	
Distribution	Location	Shape	Scale	Threshold	Log-Likelihood	AD	p Value	LRT	AIC
Gamma		1.358	1282.5		-3205.7	0.699	0.084		6415.5
Weibull		1.190	1849.9		-3206.7	0.871	0.026		6417.4
Gamma - Three Parameter		1.374	1269.9	-3.155	-3205.7	0.652	0.105	0.777	6417.4
Weibull - Three Parameter		1.184	1844.0	2.734	-3206.6	0.896	0.023	0.662	6419.2
LogNormal - Three Parameter	7.383		0.700	-300.7	-3209.0	0.553	0.153	0.000	6424.1
LogLogistic - Three Parameter	7.319		0.438	-197.2	-3213.6	0.982	0.006	0.000	6433.1
Exponential - Two Parameter			1736.9	4.689	-3214.8	5.856	<0.001	0.152	6433.5
Exponential			1741.6		-3215.8	5.736	<0.001		6433.6
LogLogistic	7.148		0.556		-3221.9	2.637	<0.005		6447.8
Largest Extreme Value	1124.8		965.5		-3234.4	2.620	<0.01		6472.7
LogNormal	7.051		1.058		-3239.9	5.891	0.000		6483.8
Normal	1741.6		1552.5		-3331.3	15.07	0.000		6666.6
Smallest Extreme Value	2656.4		2542.8		-3496.3	44.68	<0.01		6996.6

Curve fitting summary table for indirect WUI

Descriptive Statistics									
	Count	Mean	StDev	Median	Min	Max	Skew	Kurt	
	380	3599.8	3535.2	2492.7	2.939	23825	2.339	7.327	
Distribution	Location	Shape	Scale	Threshold	Log-Likelihood	AD	p Value	LRT	AIC
LogNormal - Three Parameter	7.921		0.836	-265.6	-3481.1	0.243	0.766	0.000	6968.2
Gamma		1.278	2816.1		-3485.1	1.294	<0.005		6974.1
Gamma - Three Parameter		1.286	2801.4	-2.505	-3485.0	1.304	<0.005	0.773	6976.0
Weibull		1.119	3762.2		-3487.6	1.830	<0.01		6979.3
LogLogistic	7.803		0.564		-3487.8	0.740	0.032		6979.5
Weibull - Three Parameter		1.117	3758.5	1.337	-3487.6	1.825	<0.01	0.820	6981.2
Exponential			3599.8		-3491.7	3.784	<0.001		6985.4
Exponential - Two Parameter			3596.9	2.939	-3491.4	4.013	<0.001	0.431	6986.7
LogLogistic - Three Parameter	7.800		0.578	2.936	-3493.0	0.820	0.019 *		6991.9
LogNormal	7.749		1.046		-3500.8	1.982	0.000		7005.6
Largest Extreme Value	2232.3		2047.1		-3531.0	6.813	<0.01		7066.1
Normal	3599.8		3530.6		-3643.5	22.39	0.000		7291.0
Smallest Extreme Value	5674.7		5511.1		-3796.6	46.64	<0.01		7597.2